RESEARCH ARTICLE OPEN ACCESS

Computational Evaluation of Blending Ratio on the Fluidised BED Gasification System-CFD Versus Test

M. Ramarao[1], [2]S.Jayakrishna [3]P.Senthilkumar [4]G.Elango [5]M.Leela Ramesh[6]S.Sathish

1(Department of Mechanical Engineering, Holy Mary institute of technology &science college of engineering, Hyderabed.)

2(Department of Mechanical Engineering, Holy Mary institute of technology &science college of engineering, Hyderabed)

3(Department of Mechanical Engineering St.Joseph of college of engineering ,Sriperumbudur.Tamilnadu

4(Department of Mechanical Engineering Krishnasamy college of engineering and technology, cuddalore,Tamilnadu)

5(Department of Mechanical Engineering, Holy Mary institute of technology &science college of engineering, Hyderabed)

[6](Department of Mechanical Engineering, Hindustan university,Chennai,Tamilnadu)

Abstract:

The objective of this work was to assess the combined effects of the Corn Stalk, wheat and coconut shell in a fluidized gasification process, where the focus was to quantify the relationships between the response variables and vital operating factors. With a view to the shortcomings of the classical "one factor-at-a-time" method in identification of the effect of experimental factors and their interactions, a statistical design of the experiment based on response surface methodology (RSM) was used. The response variables used in this work were gasification efficiency, tar yield and carbon conversion with different bed materials such as silica and limestone. Using RSM, the effects of individual operating factors and their interactions were categorically determined, which were not otherwise possible by the classical design of experiment methodology. Using the resultant response variable correlations, gas efficiencies were optimized as a function of the different blending ratios and bed materials using respectively. In order to validate the optimized parameters, a comprehensive three-dimensional numerical model is developed to simulate gasification in a fluidized bed reactor using Eulerian–Lagrangian approach. The model predicts product gas efficiency and carbon conversion efficiency in good agreement with experimental data. The formation and development of flow regimes and distributions of gas compositions inside the reactor are also discussed.

I.INTRODUCTION

An agricultural residue that could be utilized for the recovery of energy is Corn Stalk because of its reasonably high energy content (12–18 MJ/kg). Today in many countries, most of the surplus Corn

Stalks are disposed by direct burning in open heaps, which results in loss of energy as well as emission of various pollutants to the atmosphere [1–4]. Gasification as a process of converting carbonaceous materials into gaseous products using a gasifying medium such as air, oxygen, and steam has been considered as an alternative to combustion

of low density biomass materials [5]. Further, the gasification process is typically 80–85% thermodynamically efficient in converting the organic content of the feed into a fuel gas mixture

containing carbon dioxide, carbon monoxide, hydrogen, methane, excess steam and also nitrogen (if air is used as a gasifying agent), in addition to some minor organic compounds, tars, other minor components such as ammonia, and sulfur compounds. Besides, the gasification process generates a clean fuel gas which can be utilized in a combined cycle power generation system with enhanced efficiency. An integrated gasification

combined cycle system offers a generating efficiency in the order of 40%, which is higher than that for a conventional direct combustion pulverized coal fired plant (~34%) [6].

Co-gasification technology of coal and biomass offers advantages, such as reduction of air pollutants (e.g., NOx and SOx) and volatile organic compounds [7], improved gasification reactivity (alkali and alkaline earth metal in biomass ash behave as catalysts in coal gasification [8], and increase in gas yield. Thus, it is becoming increasingly important, because it allows for the use of coal in a more environmentally friendly way and contributes to the implementation of biomass gasification on a commercial scale [9]. However, with a view to enhance the reduction of air pollutants and volatile matter, co-gasification of

agro-based biomass is appreciated. Hence it tends to discover a substitute for the coal for the co gasification. Agro based biomass is the only source of carbon-based renewable fuels and the sustainable exploitation of this resource is essential to secure the energy security. Wheat husk and coconut shell are high in sulfur content and vanadium and nickel contents (EPA-regulated elements), whereas Corn Stalk are high in moisture and ash content and low in sulfur content. Blending the above three is regarded as a promising option to improve the slag flow difficulties of high ash content husk because of the relatively low ash content of coconut shell, which reduces the risk of slag plugging the reactor tapping system. Mixing biomass also helps to reduce the sulfur loading in flue gas, which in turn results in lowering downstream processing requirements [10] Blending also helps to alleviate the high Ni and V difficulties of oil sand coke gasification, such as destroying the refractory binder, slagging and fouling on economizer heat-transfer surfaces, problems with burners and the syngas cooler, and formation of low-melting-point sodium vanadate, which deposits in the syngas cooler [11]. Furthermore, there is a chance that blending coke with coal can enhanced the conversion through catalytic activity of alkali metals in coal ashes, although the results reported in the literature are not consistent in this respect. Last but not the least; blending is one of the promising options that can further help to reduce the environmental impacts and footprints of the oil and gas industry.

Modeling and simulation can also be helpful for optimizing the biomass gasifier design and its operation (start up, shutdown, etc.) with minimal temporal and financial costs [12]. The reported mathematical models for biomass gasifier are primarily classified into three groups: thermodynamic equilibrium models, kinetics models and multiphase computational fluid dynamics (CFD) models. Due to the complexity of the gasification process, i.e., involving many phases and various chemical and physical interactions among them existing work is focused on kinetics models and equilibrium models [12]. Only a few multiphase CFD trials have been reported to simulate fluidized bed biomass gasifier.

From the literature review, it is understood that there are a large number of fluidized bed biomass gasifiers developed worldwide for co-gasification; unfortunately most of these projects are struggling to reach commercialization. Very few investigations have been done related to the prediction of the gas efficiency, gas yield and tar yield , incorporating the process parameters like temperature, equivalent ratio and steam to biomass ratio alone. The main objective of this research is to develop an empirical relationship to predict the gas efficiencies with respect to blending ratio of different biomasses and also to optimize the processing parameters for the above said gasification using desirability approach, Furthermore, a three-dimensional Eulerian–Lagrangian model is developed to validate the optimized performance of the fluidized bed biomass gasification by simulating the complex granular flow and chemical reaction simultaneously. The experimental data and the predicted vales have been analyzed, compared and discussed in the present work.

1.0 EXPERIMENTAL WORK

2.1. Feedstock and inert bed materials

The feed stock selected to study the fluidized bed gasification were coconut shell, Corn Stalk and wheat husk with different biomass ratio. These biomaterials were collected from rural industries of Cuddalore district, India. The proximate and ultimate analyses of coconut shell, Corn Stalk and wheat husk used as feed stock are presented in Table 1. The inert bed materials used were silica and lime stone and its particle size distribution were selected as 0.400 mm using sieve analysis. The properties of these materials and the procedures followed in finding out physical and chemical properties are mentioned in detail. Absolute specific gravity of the selected materials was measured using specific gravity bottle method. To minimize the complexities, resulting from the non-uniform particle size distribution in the bed, the average particle diameter was used to represent the particle size. Sieve analysis is commonly used to predict the particle size distribution of the feed stock having size of 70-500 µm. The test materials were dried and then sieved in a set of standard sieves and particle size distribution was observed [12]. Using oven method (110°C till reaching standard borne dry weight), moisture content of feed stock was measured (ASTM, E – 871). Proximate composition such as volatile matter (ASTM, E – 872) and ash (ASTM, E – 830) and fixed carbon (by weight difference) was found out by ASTM procedures. The elemental composition of the feed stock was found out using Elemental Analyzer (Carlo Erba EA 1108) coupled with auto sampler AS-200 and data processor DP 200-PRC. The minimum fluidization velocity was measured using pressure drop method. U tube manometers are used to measure the pressure drop below and above the distributor plate and at different heights of fluidized bed reactor. The air velocity corresponding to the peak pressure drop gives the experimental value of minimum fluidization velocity [13].

2.2 Experimental Set up

A pilot scale fluidized bed Corn Stalk gasifier (capacity: 20 kg/h) had been developed and installed in the laboratory to carry out the experimental investigation. The schematic diagram of the setup is shown in Fig. 1. Table 2 shows the design and operating features of Fluidized Bed Gasifier. The cylindrical gasifier with 108 mm inside diameter up to a height of 1400 mm made of carbon steel material having inside refractory lining of thickness 0.1 m. The gasifier is fitted with a multiple hole distributor plate of 105 mm diameter was used for air distribution The ash discharge systems were provided for periodical disposal through the lock hopper arrangements. Silica sands and lime stone as bed materials were initially put into the gasifier through the screw feeder and air was introduced at the bottom of gasifier to maintain the bed in fluidized state. The air flow, after the discharge of blower, was controlled by a regulating valve and the flow was then estimated by an orifice meter placed in the supply pipe on the basis of pressure drops recorded across it. The orifice had been calibrated prior to the experiment with two reference instruments; namely a digital micromanometer (make: Furnace Control, England) and a thermal anemometer (make: Dantec, Denmark). The pressure drops across the orifice were recorded in the manometer and the corresponding flow rates were measured by the anemometer; the calibration curve was thus generated by plotting the flow rates along abscissa and the corresponding pressure drops along the ordinate.

During experiment, the pressure drops were noted to get the corresponding air flow rates from the curve at different equivalence ratios. External electric heating was used for preheating the bed materials as well as the refractory lining during start up. The electric heating was switched onto and the gasifier was allowed to run until the bed temperature was 450°C. The raw Corn Stalk was then fed through the under-bed feeding system having a screw feeder. The feed rate was controlled by the screw feeder fitted to a variable speed drive and it push the solid fuel immediately into the gasifier preventing pyrolysis outside the chamber. Supply of air was then regulated to maintain the desired equivalence ratio.

The cyclone at the outlet of gasifier was used to separate the solid particles from the fuel gas mixture. The bag filter placed after the cyclone further cleaned up the gas by capturing dust and other smaller particles. The water cooler and an ice trap system were used in series to cool the fuel gas to separate the tar through condensation. A second orifice meter (50 mm diameter) was positioned in the fuel gas pipe (108 mm diameter) to estimate the gas yields. The calibration of the orifice was done prior to the experimental work by following the similar procedure as it was done in case of orifice meter in airline to generate a separate calibration curve. While the gasifier was running, the pressure drops across the orifice were noted in manometer to get the corresponding gas flow rates from the curve. The flow rates thus obtained corresponding to gas temperatures was then corrected by the temperature factor to get the actual flows at NTP. Equivalence ratio is very important in gasification process as it determines the fraction of the fuel that is burnt and thereby it controls the bed temperature. It also affects the fluidization of the bed. The lower limit of equivalence ratio is decided by the minimum quantity of air required to burn a portion of the fuel to release enough heat to support the endothermic reactions, to meet the sensible heat losses in gas, char and ash, and to maintain the required bed temperature of the reactor. As Corn Stalk has high ash content, it requires larger fraction of the fuel to be burnt – this ultimately demands a higher equivalence ratio [14]. In Hartiniati et al. [15], it is reported that the equivalence ratio was maintained between 0.30 and 0.48 during experimentation in a pilot scale fluidized bed gasifier fueled by mixture. Later on, Mansaray et al. [16] also investigated the Corn Stalk and wheat husk gasifier performance in a fluidized bed system by varying the equivalence ratio at 0.25, 0.30 and 0.35. In view of these observations, the gasifier was operated with equivalence ratios of 0.20-0.50 in the present investigation to get the experimental results.

2.3 Experimental Design Matrix

From the studies [17-26] producer gas and the carbon conversion efficiency have been identified. The biomasses such as coconut shell, Corn Stalk and wheat husk are used in the present investigation. Owing to a wide range of factors, the use of five factors and central composite rotatable design matrix was chosen to minimize number of experiments. The number of tests required for the CCRD includes the standard 2k factorial with its origin at the center, 2k points fixed axially at a distance, say α, from the center to generate the quadratic terms, and replicate the tests at the center; where k is the number of variables. The axial points are chosen such that they allow rotatability, which ensures that the variance of the model prediction is constant at all points equidistant from the design center. By adding axial points which extend, the design will provide protection against the curvature from twisting. Hence, the design was extended up to ± α (axial point). The value of α is chosen to maintain rotatability. To maintain rotatability, the value of α depends on the number of experimental runs in the factorial portion of the central composite design, which is given by Equation (3.1)

$$\alpha = [\text{number of factorial points}]1/4 \quad (3.1)$$

If the factorial is a full factorial, α is evaluated from the Equation (3.2)

$$\alpha = [23]1/4 = \pm 1.682 \quad (3.2)$$

It can be noted that when $\alpha > 1$, each factor is run at five levels (-α, -1, 0, +1, +α) instead of the three levels of -1, 0, and +1. The reason for running the central composite designs with $\alpha > 1$ is to have a rotatable design. However, the factorial portion can also be a fractional factorial design of resolution. The center values for the variables were carried out at least six times for the estimation of error, and single runs for each of the other combinations. Replicates of the test at the center are very important as they provide an independent and more uniform estimate of the prediction variance over the entire design. Table 3.4 presents the ranges of factors considered. For the convenience of recording and processing the experimental data, the upper and lower levels of the factors are coded as +1.682 and -1.682 respectively. The coded values of any intermediate value can be calculated by using the Equation (3.3)

$$X_i = 1.682\,[2X - (X_{max} - X_{min})] / (X_{max} - X_{min}) \quad (3.3)$$

where,

Xi is the required coded value of a variable X, and X is any value of the variable from Xmin to Xmax

Xmin is the lower level of the variable.

Xmax is the upper level of the variable.

Xmax is the upper level of the variable.

Design matrix consisting of 20 sets of coded conditions (comprising full replication 8 factorial points, 6 corner points and six center points) was chosen in this investigation. Table 3 represents the ranges of factors considered, and Table 4 shows the 20 sets of coded and actual values with experimental results.

2.5 Experimental Testing

During experimentation, special care was taken to maintain the desired bed temperatures as the selected feedstock were coconut shell, Corn Stalk and wheat husk. One of the important features of biomass gasification is that the bed temperature can be kept as low as 700–900°C, thereby preventing sintering and agglomeration of this ash which would otherwise cause serious operational problems during the conversion process [27]. The upper temperature is fixed by slagging phenomena which primarily depends upon the ash composition and the reaction atmosphere (like oxidation or reduction). Above this temperature, silica and potassium oxide in ash fuses on the surface of Corn Stalk char particles forming a glass-like barrier that prevents the further reaction of the remaining carbon [28]. Some studies [29, 30] also indicate that oxidation of biomasses at a temperature higher than 900°C results in a physical structural transformation of silica from its original amorphous state to a crystalline state thereby encapsulating residual carbons. Once the structural changes of silica occurs, the combined carbon becomes unavailable for further oxidation reactions even at higher temperatures. In view of this, the gasifier was operated in the range of 700–950°C when the experiments were carried out with equivalence ratio 0.2 and 0.5.

The gasification temperature was raised up to 700°C only in case of equivalence ratio of 0.25. The gasifier temperatures were recorded using Ni–Cr–Ni thermocouples with a digital display system. The gas sampling system was composed of probes fitted with septum. The sampling point was located at the outlet pipe of gasifier. The gas sampling probe made of glass was 50 mm in diameter and 500 mm in length. A syringe of volume capacity of 10 ml was used to collect the gas sample. The sample was analyzed in the Gas Chromatograph (Make – Chemito, model – GC1000) to get the raw experimental data and those were compared with the predicted values of the developed model. The energy content of the gas is assessed through the variable CCE (carbon conversion efficiency). This variable represents the ratio between the energy content of the permanent gas and the energy content of the initial biomass feedstock without taking into account the heat input in the reactor:

$$CCE = [(M_{CO\%} + M_{CH4\%} + M_{CO2\%}) * 12] / M_{feed\ rate}$$

$$GE = HHV_{gas} / HHV_{biomass}$$

where HHV for the biomass is calculated from;

$$HHV_{biomass} = (CO\% * 3018 + H_2\% * 3052 + CH_4\% * 9500)*0.01*4.1868\ (kJ/Nm^3)$$

At the end of the experiment the residual tar were weighed and stored in a sealed recipient for further characterization. The tar yield is expressed as the ratio of the residual tar to the initial mass of biomass

$$Y_{Tar}\% = [(M_{Tar}) / (M_{biomass})] \times 100$$

2.6 Computational domain, initial and boundary conditions

Computational Analysis is further enhancing to correlate the experimental and statistical evaluation. The validation among the experimental, statistical computational analysis gives a better understanding the gasification behavior of biomass blends. The Eulerian–Eulerian model was implemented using the commercially available Computational Fluid Dynamics software FLUENT12.0 (ANSYS, Inc., USA). The reactor domain has been discretized with a uniform Cartesian grid. The grid cell size is 4 mmx2mmx8.75 mm (Δx, Δy & Δz). Inlet and boundary conditions are modeled to match the experiments as close as possible. Heated air flows through the distributor with 25 holes. The biomass feeding rate from the experiment is transformed into the particle injection rate. At the outlet, gas phase adopts out-flow boundary condition and outlet pressure is fixed to atmosphere. The reactors is filled at the beginning of the calculation with 30 g silica sand and lime stone with the volume fraction 0.48 each separately [31]. To prevent excessive compression of particles, the solid close pack volume fraction is set as 0.5. The initial conditions are corresponding to the conditions of the real reactor after heated up with pure nitrogen. The particle normal-to-wall momentum retention coefficient is 0.2 and the tangent–to-wall retention coefficient is 0.99. The time step of 2.0×10^{-4}s is used. Equivalence ratio (ER), and average relative error (ARE) are referred from the previous literature [32, 33]. For modeling of solid particles the following assumptions have been made as the gas phase species are ideal gas, particles are assumed as isotropic material and the properties change along the radius (for sphere particles) and the solid and gas (inside the particle) are in local thermal equilibrium.

3.0 RESULTS AND DISCUSSION

3.1 Developing Empirical Relationship

In the present investigation, to correlate the process parameters and the quality of the producer gas, a second order quadratic model was developed. In this study, the RSM provides a quantitative form of relationship between the desired response (Quality of the Producer gas) and the independent input variables (Biomass ratio), Coconut shell (C), Corn Stalk (R), and Wheat husk (W), and can be expressed as a function, as in Equation (3)

Quality of the Producer gas (Q) = f (C, R, W)..... (3)

The empirical relationship must include the main and interaction effects of all factors and hence the selected polynomial is expressed as follows:

$$Y = bo + \sum bi\ xi + \sum bii\ xi^2 + \sum bij\ xi\ xj \quad ..... (4)$$

For three factors, the selected polynomial could be expressed as

$$\text{Quality of the Producer gas (Q)} = \{ b_0 + b_1 (C) + b_2 (R) + b_3 (W) + b_{11} (C^2) + b_{22} (R^2) + b_{33} (W^2) + b_{12} (CR) + b_{13}(CW) + b_{23} (RW) \} \quad ..... (5)$$

where b_0 is the average of responses () and b_1, b_2, b_3… b_{11}, b_{12}, b_{13}… b_{22}, b_{23}, b_{33}, are the coefficients that depend on their respective main and interaction factors, which are calculated using the expression given below,

$$B_i = (\sum (Xi,Yi))/n \quad .... (6)$$

Where 'i' varies from 1 to n, in which Xi the corresponding coded value of a factor and Yi is is the corresponding response output value (Biomass Blend) obtained from the experiment and 'n' is the total number of combination considered. All the coefficients were obtained applying central composite rotatable design matrix including the Design Expert statistical software package. After determining the significant coefficients (at 95% confidence level), the final relationship was developed including only these coefficients. The final empirical relationship obtained by the above procedure to estimate producer gas generation, tar yield and carbon conversion efficiency of biomass blend under fluidized bed gasification is given below;

Gas Efficiency (Silica)

Producer Gas (GE S) = +82.338 -2.768 *(C) -0.570 *(X) -0.569 (W) -5.185×10^{-3} *(CX) + 0.0126 (CW) +0.013 *(XW) + 0.079* (C^2) +3.150x 10^{-3} (X^2) +0.054*(W^2)

Gas Efficiency (Limestone)

Producer Gas (GE L) = +72.555 -2.546*(C) -0.528 *(S) -0.397 (X) -4.305 x 10^{-3} *(CX) + +9.277x 10^{-3}* (CW) +9.446x 10^{-3}* (XW) + 0.072* (C^2) +3.208x $^{10-3}$ (X^2) +0.053*(W^2)

Carbon Conversion Efficiency (Silica)

Producer Gas (CCE S) = +86.323 -2.759*(C) -0.557*(X) -0.539(W) -5.185x 10^{-3} *(CX) + 0.0126* (CW) +0.013* (XW) + 0.078* (C^2) +2.887x $^{10-3}$ (X^2) +0.052*(W^2)

Carbon Conversion Efficiency (Limestone)

Producer Gas (CCE L) = + 90.192 -2.759*(C) -0.557*(X) -0.539(W) -5.185x 10^{-3} *(CX) + 0.0126*(CW) +0.013*(XW) + 0.078*(C^2) +2.882x 10^3 (X^2) +0.052*(W^2)

Tar yield (Silica)

Producer Gas (TY S) = +11.017 -0.499 *(C) -0.138 *(X) -0.163 (W) + 5.342 x 10^{-4} *(CX) -1.236x10^{-3} (CW) + 8.975x 10^{-4} * (XW) + 0.014* (C^2) +1.384x 10^{-3} (X^2) + 0.015* (W^2)

Tar yield (Limestone)

Producer Gas (TY L) = +14.537 - 0.499 *(C) -0.138 *(X) -0.163 (W) -5.342 x 10^{-4} *(CX) -1.236x10^{-3} (CW) +8.975x 10^{-4} * (XW) + 0.014* (C^2) + 1.384x 10^{-3} (X^2) + 0.015* (W^2)

The Analysis of Variance (ANOVA) technique was used to find the significant main and interaction factors. The results of second order response surface model fitting as Analysis of Variance (ANOVA) are given in the Table 5. The determination coefficient (r^2) indicated the goodness of fit for the model. The Model F-value of (CCE_L = 5.76, CCE_S = 5.76, GE_L = 5.88, GE_S = 6.24 , TY_S = 4.66, TY_L = 4.66, implies the model is significant. There is only a 0.01% chance that a "Model F-Value" this large could occur due to noise.

3.2 Optimizing the Diffusion Bonding Parameters

In this investigation, the RSM was used to optimize the process parameters for biomass gasification. RSM is a collection of mathematical and statistical techniques that are useful for designing a set of experiments, developing a mathematical model, analyzing for the optimum combination of input parameters, and expressing the values graphically [19]. To obtain the influencing nature and optimized condition of the process on shear strength and bonding strength, the surface and contour plots, which are the indications of possible independence of factors, have been developed for the proposed empirical relation by considering two parameters in the middle level and two parameters in the X- and Y-axes as shown in Fig. 2, 3 and 4 respectively. These response contours can help in the prediction of the response for any zone of the experimental domain [28].The apex of the response plot shows the maximum achievable gas efficiency, carbon conversion efficiency and lowest tar yield.

The gasification behavior of the biomass blends over different combinations of the independent variables is shown through a two-dimensional view of the contour plots. The contour plots are represented as a function of two factors at a time, holding the other factors at a fixed level. All the contour plots revealed that at low and high levels of the variables, the response is minimal; however, it is noted that there existed a region with a color difference, where neither an increasing nor a decreasing trend in the gasification behavior was observed. This phenomenon confirms that there was an optimum for the gasification mixing variables, in order to maximize the gasification capacity. Figure 2 shows the interaction effects of the Corn Stalk and the coconut shell on the gasification behavior of the biomass blends. It is observed that, the stationary point is far outside the region of exploration for fitting the second order model. The contour surface is assumed to be a rising ridge. In this type of ridge system, the least or most number of contours was assumed to be an optimal degree of solution. Elliptical contours exist in the interaction plots for all the gasification tests. It can be seen that an inverse relationship between Corn Stalk and the coconut shell on the gasification behavior of the biomass blends was found in all the plots. Figure 2 shows the effect of Corn Stalk and the coconut shell on the gasification behavior of the biomass blends.

It was observed that on increasing Corn Stalk and the coconut shell on the gasification behavior of the biomass blends, the gas efficiency increases. It was authenticated by the fact that the interaction between Corn Stalk and the coconut shell on the gasification behavior of the biomass blends shows an appreciable level of significance. Also it suggested that, the Corn Stalk was more sensitive than coconut shell on the gasification behavior of the biomass blends. Thus, the contour plots, clearly show the effect of gasification behavior of the biomass blends; and independently show that the gas efficiencies increased on increasing Corn Stalk and the coconut shell. Figure 3 shows the interaction effects of the coconut shell and the wheat husk on the gasification behavior of the biomass blends. It shows the wheat husk also played an important role on the gasification behavior of the biomass blends; this was evident from the equation and contour plots. The interaction between the coconut shell and the wheat husk was distorted, which was reflected by the corresponding p-values, but, it was clear that, the wheat husk was more sensitive than the coconut shell. Further, it was seen that, on increasing the wheat husk and coconut shell the gasification behavior increase. Circular contours were found and the optimal value falls at the center of the concentric circles. Fig. 4 shows the effects of the Corn Stalk and the wheat husk on the gasification behavior of the biomass blends. It was observed that the interaction of the Corn Stalk and the wheat husk was appreciably significant on the gasification behavior of the biomass blends. This was evident from the corresponding p-values, and deduced from the curvature of the contour. It was noted that, on the gasification behavior of the biomass blends especially carbon conversion efficiency decreased with increasing Corn Stalk and with the increment in the wheat husk. The trend observed in the other responses was different as increases with increase in the composition and blends. As an interactive factor, the Corn Stalk is more sensitive than the wheat husk during the gasification.

In order to optimize the process parameters to maximize the gasification efficiency, a combined analysis is done based on their desirability criteria. Desirabilities range from zero to one for any given response. The program combines the individual desirabilities into a single number and then searches for the greatest overall desirability. A value of one represents the ideal case. A zero indicates that one or more responses fall outside desirable limits. A total number of cycles (10 cycles) per optimization were given. This is a complex combination of response surfaces, increasing the number of cycles will give more opportunities to find the optimal solution. The Duplicate solution filter establishes the epsilon (minimum difference) for eliminating duplicate solutions. The program using Design Expert software, randomly picks a set of conditions from which to start its search for desirable results. Multiple cycles improve the odds of finding multiple local optimums, some of which will be higher in desirability than others. After grinding through 10 cycles of optimization, the results appear as the most optimal parameters are coconut shell with 26.80%, Corn Stalk with 4.58% and wheat husk with 15.34% with the desirability of 0.70. Fig. 5 shows histogram of desirability is generated for the optimal solution of process parameters found via numerical optimization.

3.3 Computational Validation

In order to validate the computational and statistical model and to verify the accuracy of the simulation, the predicted results are compared with experimental data measured further shown in Table 6. It is observed that in the fluidized bed, air was used as the fluidizing agent and introduced into the reactor below the distributor. The system contains four types of particles: silica sand, limestone, carbon and ash. Flow patterns transformation colored with particle volume fraction is shown in Fig. 6. The large bubbles or intense slugs (void structures) form when gas flows up the distributor. The growth can be observed whereas the coalescence and eruption are difficult to identify because of the high gas velocity. Particles gradually move up driven by gas-particle interactions. After t = 0.4 s, the particle profile shows the relatively steady state. The particle volume fraction decreases along the reactor height.

3.3.1 Effect of Coconut shell

Two series of tests have been performed with silica and limestone as bed material. The main difference in both series is the blending ratio (BR) used. As a biomass blend, coconut shell plays a vital role in biomass gasification process. In this present work, though it was an autothermal gasifier, the fuel gas was evaluated at various intermediate coconut shell ratio in the biomass blend until it reached the maximum ratio for a given Corn Stalk and wheat husk. Table shows the experimental data of gas species taken at coconut shell ratio between 0 to 30% of the total blend. It was seen that the calculated values fits good from the experimental data, although the similar trends (increase or decrease) were observed regarding the changes of species concentrations. It is found that with the increase of coconut shell ratio, the carbon conversion efficiency, gas efficiency and tar yield increases. It is noted that for both the bed materials the carbon conversion efficiency, gas efficiency and tar yield increases with the increase in coconut shell ratio. This may be explained with Le Chatelier's principle which states that higher concentration of coconut shell ratio favors the reactants in exothermic reactions and the products in endothermic reaction. Therefore, the endothermic reaction was strengthened with increasing coconut shell ratio, which resulted in more H_2 and less CH_4 concentrations.

It is well-known how the addition of limestones to the bed changes the product distribution in processes of combustion, incineration, gasification, and pyrolysis of biomass. These calcinated solids mainly react with some contaminants like HCl, SO_2, PAHs, etc., and eliminate them in some extent from the fuel gas. The in-bed use of limestone in biomass gasification seems also to have found commercial application. Many researches [34, 35, 36] used in-bed limestone and dolomite, respectively, for biomass gasification with steam, and in the earlier research [34] dolomite for biomass gasification with air but under pressure. Since there was some lack of knowledge in biomass gasification with air at atmospheric pressure, hence the present research was made for this purpose. All the runs were made with silica and limestone to study the effect of biomass blending ratio on the gas efficiency, carbon conversion efficiency and tar yield. The biomass blends used with the limestone bed materials shows better performance than the silica bed materials. This is due to the low heating value (LHV) of the gas decreases somewhat with lime stone. This is attributed to the in-bed tar elimination reactions which increase the H_2, CO, and CH_4 contents in the producer gas. For the just said reasons, gas yield increases with limestone bed materials. Thus it reduces the tar yield because the rates of the in-bed char elimination reactions (partial oxidation, steam, and dry (CO_2) gasification, etc.) increase on limestone bed materials. As is observed, the carbon conversions of the producer gas with limestone bed materials vary significantly as tabulated in the Table 4. The high reactivity of limestone can be explained by its high initial porosity. Limestone has also earlier been found to behave differently than the other silica under gasification. When comparing the porosity with the reactivity of the sorbents, the higher the porosity, the higher the final conversion. This is in agreement with the work of previous research [37]. Due to the decomposition of CaCO3 to CaO, the porosity of the limestone was increased, thus increasing the conversion rate

3.3.2 Effect of Corn Stalk

Corn Stalk is a predominant biomass used for the gasification. Table 4 shows both theoretical values and experimental data of gas species taken at Corn Stalk ratio between 0 to 60% of the total blend. The influences of addition of rice clearly demonstrated that, because of the thermal instability of carbon, a higher percentage of Corn Stalk results in a lesser degree of carbon conversion in both silica and limestone bed material. However, the carbon conversion with lime stone as a bed material is comparatively higher than the silica bed materials. Compared to thermodynamic equilibrium the syngas contains less CO. The syngas also contains 1.3% CH_4 which is not predicted at all at equilibrium (~10-4 %). A possible explanation could be that the heterogeneous reactions involved in char gasification are too slow to be completed within the residence time of the reactor at the current gasification conditions. This will thereby result in less CO_2 and CO. The syngas can also have become shifted in the quench, which could also explain differences between the measured syngas composition after the quench compared to the syngas composition at equilibrium. Generally, increasing the Corn Stalk will increase the gas efficiency since the heating value of the produced gas will increase with pressure [38] as a result of CH_4 production through the steam reforming reaction. On the other hand, with silica bed material increasing Corn Stalk will decrease the heating value of produced gas and hence lower the gas efficiency.

In terms of tar yield, with the increase of Corn Stalk, the tar yield increases. On comparing the bed materials, the limestone bed material possesses lesser tar yield. According to the course of the catalytic reaction, the tar needs to be absorbed first by the active sites of the bed material, which is not only affected by the physical properties of the bed material but also by the transfer behavior of the volatiles. In this experiment, calcium oxide was fine and was prone to enter the freeboard, which had no bubbles, with good contact between the bed material and the tar; thus, the tar cracking would be improved. The tar conversion increases apparently as Corn Stalk rises. The addition of Corn Stalk favors the conversion of tar. It is well-known that the polarities of the active site of silica could not affect the π-electron cloud's stability of condensed aromatic compounds in tar, so the addition of silica decelerates the cracking of condensed aromatic compounds and results in the quick decrease of tar yield.

3.3.3 Effect of Wheat husk

Major constituents of wheat husk such as hydrogen, nitrogen, oxygen and minerals such as calcium. It is observed for each gasification trial and are represented in Table 4. The data with the increase of wheat husk, the carbon conversion efficiency, gas yield increases. High reactivity of biomass causes an increase in volatile matter, which subsequently gets converted to free radicals and therefore improves the decomposition, oxidation and gasification reactions. It is reported that due to both high reactivity and high contents of hydrogen and oxygen in biomass, carbon conversion during co-gasification is greater than other biomass gasification alone and this tends to increase with increasing biomass content in the fuel. It is reported that higher conversion of fuel during co-gasification causes an increase in the gas yield [39]. In the co-gasification, higher gas yield is reported with an increase in wheat husk composition in the fuel as a consequence of higher concentration of hydrocarbons. In earlier research [39], gas yield increases with an increase in biomass ratio due to transfer of hydrogen radicals from biomass that causes more decomposition of fuel. In addition, gas yield reaches to a maximum value when the fuel blend consists of 30% of wheat. This is due to the reaction of oxygen content and carbon content in biomass, CO increases. They also state that by increasing the cracking of tar by means of volatiles present in biomass such asH_2O andH_2 radicals, CH_4 increases. The wheat husk as a biomass plays a key role in the production of tar during co-gasification in comparison with other feedstock components. It is observed that in co-gasification of wheat husk with Corn Stalk with, tar contents are decreased, although it is reported that the structure of tar that is formed is harder than that formed by individual biomass. It is also claimed that the synergetic effects of wheat husk with coconut shell causes a decrease in tar contents during cogasification. It is also observed that the use of high air/fuel ratio with higher contents of biomass during co-gasification, due to which less tar yield is produced. It is further confirmed that tar production in co-gasification of biomass is lower than in the gasification of individual fuels as a result of synergetic effects between both fuels. The investigation of wheat contents in cogasification shows a decrease in tar production, when wheat proportion increases in fuel blends as wheat has less complex structure than biomass [40].

5.0 CONCLUSIONS

1. The present study was focused on the co-gasification of biomass blends in a pilot

scale fluidized bed reactor installed in the laboratory. The gasifier was operated at bed temperatures ranging from 750 °C to 950 °C with varying equivalence ratios of 0.35 to investigate the fuel gas compositions.

2. The empirical relation was developed in order to quantify the gas efficiency of fuel gas. This model gave results with high accuracy showing similar trends in predicting the variation of gas species concentrations in line with experimental data.
3. It was noticed that the carbon conversion efficiency, gas efficiency and tar yield increases with the increase in Corn Stalk, wheat husk and coconut shell. However, with the increase of Corn Stalk, the carbon conversion efficiency reduces.
4. On comparing the efficiency of the producer gas, the lime stone bed material shows better performance than the silica bed material.

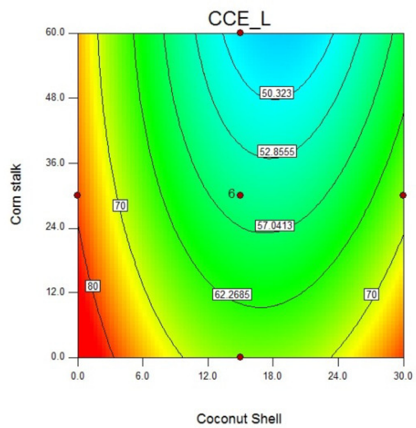

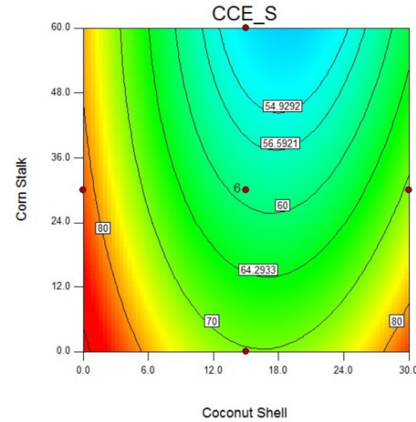

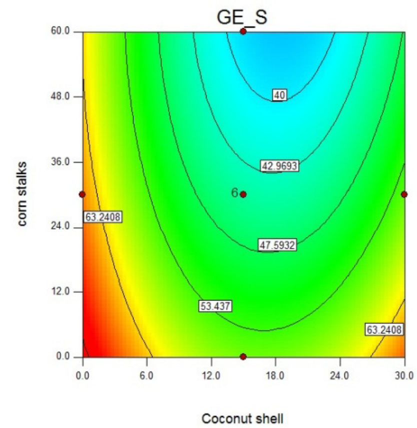

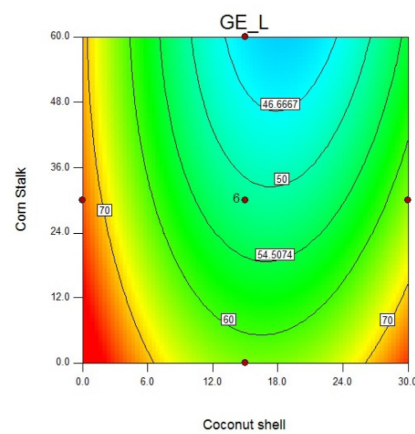

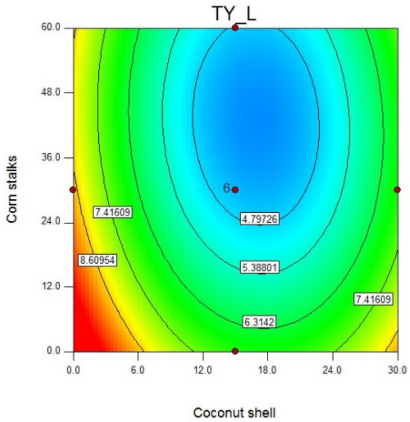

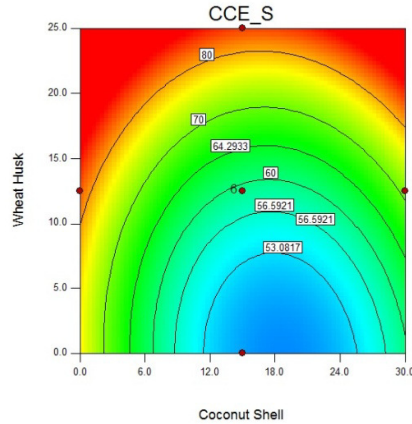

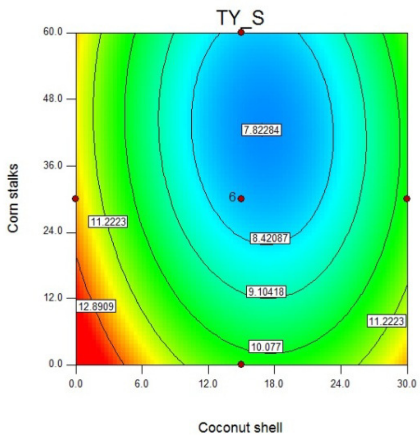

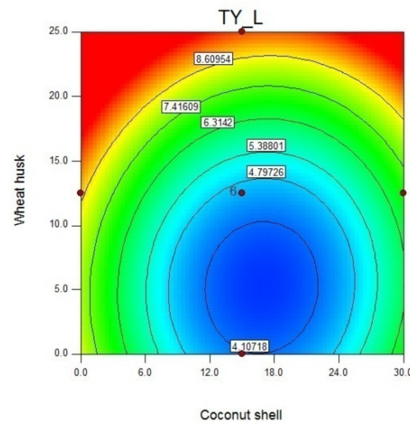

Fig. 2 Response Contour Plots Showing the Effect of Interaction Factors (Coconut Shell & Corn Stalks)

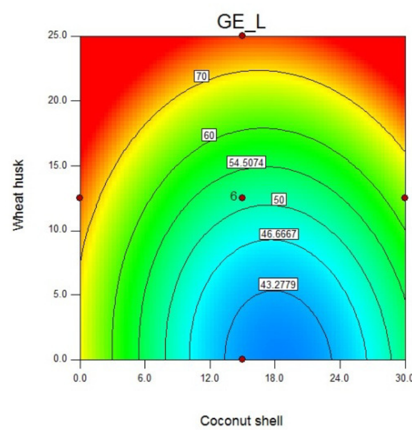

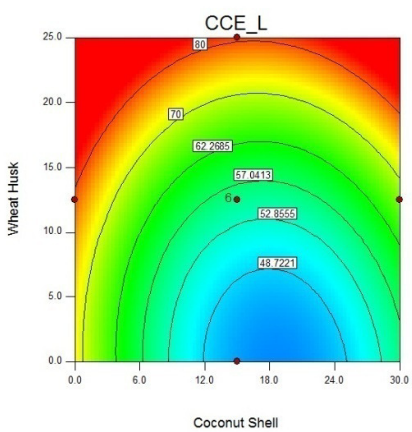

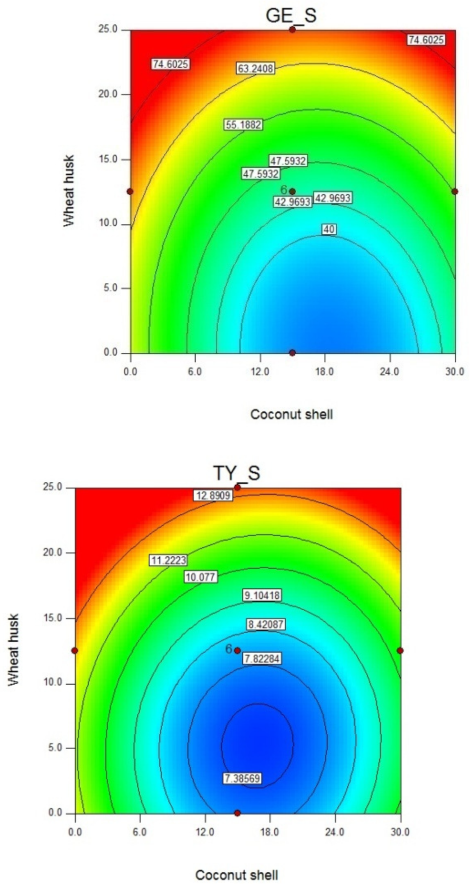

Fig. 3 Response Contour Plots Showing the Effect of Interaction Factors (Coconut Shell & Wheat husk)

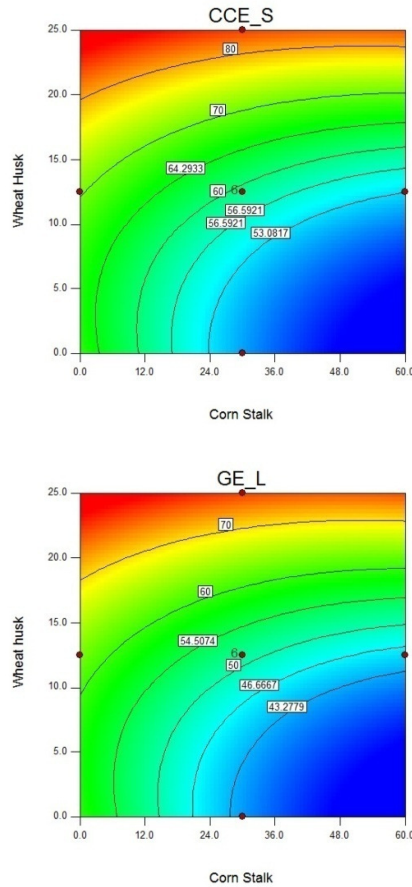

THT

FIG4:RESPONSE CONTOUR PLOTS SHOWING THE EFFECT OF INTERACTIONFACTORS (CORN STACK&WHEAT HUSK)

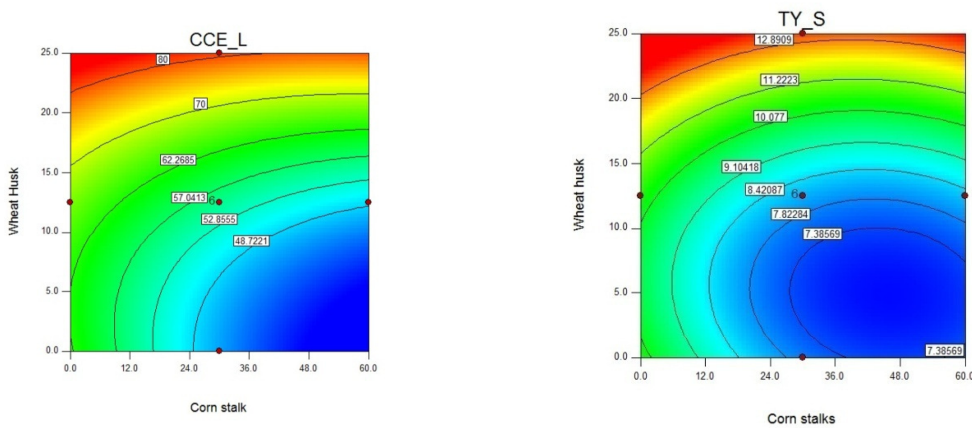

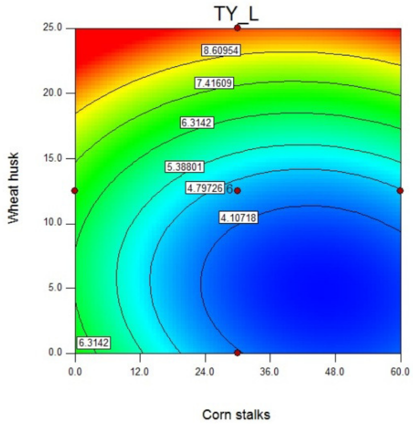

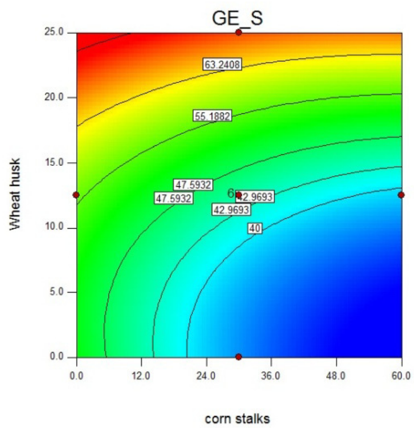

REFERENCES

1. Bridgwater, A.V.: The technical and economic feasibility of biomass gasification for power generation. Fuel. **74(3)**, 631–53 (1995).
2. Boateng, A.A., W.P. Walawender, L.T Fan and C.S.Chee : Fluidized bed steam gasification of rice hull. Bio resource Technology. **40(2)**, 235–9 (1992).
3. Beagle, E.: Corn Stalk conversion to energy, In Agricultural services bulletin. 31. Rome, Italy. FAO (1978).
4. Luan, T.C. and T.C. Chou: Recovery of silica from the gasification of Corn Stalks/coal in the presence of a pilot flame in a modified fluidized bed. Ind Eng Chem Res. **29** **(9)**. 1922-1927 (1990).
5. Ghaly, A.E., A.M. Al-Taweel and Mackay: GDM project report renewable energy division. Canada, Ottawa, Ontario: Energy Mines and Resources; 1986.
6. Schimmoller, B.K.: Coal gasification striking while the iron is hot. Power Eng. 30–40 (2005).
7. Jones J. M., M.Kubaki, K.Kubica K., A.B. Ross and A.Williams: Devolatilization characteristics of coal and biomass blends. J. Anal. Appl. Pyrolysis, **74,** 502–511 (2005).
8. Rizkiana, J., G. Guan, W.B.Widayatno, X. Hao X. Li, W. Huang and A. Abudula: Promoting effect of various biomass ashes on the steam gasification of low-rank coal. Appl. Energy, **133**, 282–288 (2014).
9. Hernandez, J.J., G. Aranda-Almansa and C.Serrano: Co-gasification of biomass wastes and coal–coke blends in an entrained flow gasifier: An experimental study. Energy Fuels, **24**, 2479–2488 (2010).
10. Peter, M.K.: Energy production from biomass (part 2): Conversion Technologies. Bioresource Technology, **83 (1)** 47–54 (2002).
11. Sims, REH: Bioenergy to mitigate for climate change and meet the needs of society, the economy and the environment. Mitigation and Adoption Strategies for Global Change, **8:** 349–370 (2003.).
12. Ahmed, T.Y., Ahmad, M.M., Yusup, S., Inayat, A., Khan, Z., 2012. Mathematical and computational approaches for design of biomass gasification for hydrogen production: A review. Renewable and Sustainable Energy Reviews 16, 2304–2315.
13. Lin, C.L., M.L. Wey and S.D. You: The effect of particle size distribution on minimum fluidization velocity at high temperature. Powder Technol.**126,** 297–301(2002).
14. Natarajan, E., A. Nordin and A.N.Rao: Overview of combustion and gasification of ricehusk in fluidized bed reactors. Biomass Bioenergy. **14(5/6)**, 533–46 (1998).
15. Hartiniati, A., A.Soemardjo and M.Youvial: Performance of a pilot scale fluidized bedgasifier fuelled by Corn Stalks. In: Proceedings of international conference onpyrolysis and gasification, 257–63 (1989).
16. Bin ZainalAlauddin, Z.A., L. Pooya, M. Mohammadi and A.R. Mohamed: Gasification of lignocellulosic biomass in fluidized beds for renewable energy development. Areview.Renewable and Sustainable Energy Reviews **14**, 2852–2862 (2010).

17. Mansaray, K.G., A.E. Ghaly, A.M. Al-Taweel, F. Hamdullahpur and Ugursal : Air gasification of Corn Stalk in a dual distributor type fluidised bed gasifier. Biomass Bioenergy. **17**, 315–332 (1999).
18. Simin Shabani, MojtabaAghajani Delavar and Mohammadreza Azmi : Investigation of biomass gasification hydrogen and electricity co-production with carbon dioxide capture and storage, international jornal of hydrogen energy **38**, 3630-3639 (2013),
19. Koc, R., N.K. Kazantzis and Y. Hua Ma: A process dynamic modeling and control framework for performance assessment of Pd/ alloy-based membrane reactors used in hydrogenproduction. Int J Hydrogen Energy **36**, 4934-51.(2011)
20. Mathieu, P. and R. Dubuisson: Performance analysis of a biomass gasifier. Energy Convers. Manage. **43**, 1291–1299 (2002).
21. Lin, C.L., M.L. Wey and S.D. You: The effect of particle size distribution onminimum fluidization velocity at high temperature. Powder Technol. **126** (2002), 297–301.
22. Drift, A.V., J. Doorn and J.W. Vermeulen: Ten residual biomass fuels for circulating fluidized-bed gasification. Biomass Bioenergy **20**, 45–56 (2009).
23. Luoa, S., B. Xiao, Z. Hua, S. Liua, Y. Guana and L. Caia : Influence of particle size on pyrolysis and gasification performance of municipal solid waste in a fixedbed reactor. Bioresour Technol.**101(16)**, 6517–6520 (2010).
24. Susana Martı´nez-Lera and Jose´ TorricoJavier Pallare´s Antonia Gil: Design and first experimental results of a bubbling fluidized bedfor air gasification of plastic waste, J Mater Cycles Waste Manag. **15**, 370–380(2013)
25. Risberg M., Ohrman O.G.W., Gebart B.R., Nilsson P.T., Gudmundsson A. and Sanati M. Influence from fuel type on the performance of an air-blown cyclone gasifier, Fuel 116, 751–759 (2014).
26. Mansaray, K.G., A.E. Ghaly, A.M Al-Taweel, F. Hamdullahpur and V. Ugursal: Air gasification of Corn Stalk in a dual distributor type fluidized bed gasifier. Biomass Bioenergy.**17**, 315–32 (1999).
27. Kaupp Albrecht : Gasification of rice hulls. Theory and practices. Deutsches Zentrum Fuer Entwicklungs Technologien (GATE): Eschborn; (1984).
28. Schiefelbein, G.F.: Biomass thermal gasification research, recent results – UnitedStates DOE's research program. Biomass **19**, 145–59 (1989).
29. Bin Zainal Alauddin Z.A., L. Pooya, M. Mohammadi and A.R. Mohamed: Gasification of lignocellulosic biomass in fluidized beds for renewable energy development, Renewable and Sustainable Energy Reviews **14**, 2852–2862 (2010).
30. Kurkela, E.; P. Stahlberg: Air Gasification of Peat, Wood and Brown Coal in Pressurised Fluidized Bed Reactor. I. Carbon Conversion, Gas Yield, and Tar Formation. Fuel Process. Technol. **31**, 1-21 (1992)
31. Wang, X.F., Jin, B.S., Zhong, W.Q., 2009. Three-dimensional simulation of fluidized bed coal gasification. Chemical Engineering and Processing 48, 695–705.
32. Buragohain, B., Mahanta, P., Moholkar, V.S., 2012. Performance correlations for biomass gasifiers using semi-equilibrium non-stoichiometric thermodynamic models. International Journal of Energy Research 36, 590–618.
33. Nikoo, M.B., Mahinpey, N., 2008. Simulation of biomass gasification in fluidized bed reactor using ASPEN PLUS. Biomass and Bioenergy 32, 1245–1254
34. Corella, J., M. P Aznar, J. Delgado, E. Aldea and P. Martı´nez, : Fuel and Useful Gas by Steam Gasification of Biomass in Fluidized Bed Followed by Tar Cracking Fluidized Bed of Dolomite/ Limestone/ Magnesite. In Biomass for Energy Industry and Environment (6th EC Conference); Grassi, G., et al., Eds.; Elsevier Applied Science: London, pp 714-721 (1992).
35. Walawender, W. P., D. Hoveland and L. T. Fan : Steam Gasification of Alpha Cellulose in a Fluid Bed Reactor. In Fundamentals of Thermochemical Biomass Conversion; Overend, R. P., et al., Eds.; Elsevier Applied Science: London; pp 897-910 (1985).
36. Illerup, J. B., K.Dam-Johansen and Lunden, K; High-Temperature Reaction between Sulfur Dioxide and Limestone-VI. The Influence of High Pressure. Chem. Eng. Sci., **48**, 2151-2157 (1993).
37. Mathieu, P. and R.Dubuisson : Performance analysis of a biomass gasifier. Energy Convers.

Manage..Eqivalent ratio & Feed rate. **43**, 1291–1299 (2002).
38. Fermoso, J, B. Arias, M.V. Gil, M.G. Plaza, C. Pevida and JJ Pis :. Cogasification of different rank coals with biomass and petroleum coke in a high-pressure reactor for H2-rich gas production. Bioresource Technol **101(9)**:3230-5 (2010).
39. Seo, M.W., J.H. Goo, S.D. Kim, S.H. Lee and Y.C. Choi:. Gasification characteristics of coal/biomass blend in a dual circulating fluidized bed reactor. Energy Fuel;24:108-18 (2010).
40. Collot, A.G, Y. Zhuo, D.R. Dugwell and R. Kandiyoti Co-pyrolysis and co-gasification of coal and biomass in bench-scale fixed-bed and fluidised bed reactors. Fuel; 78(6):667-79 (1999).

43.

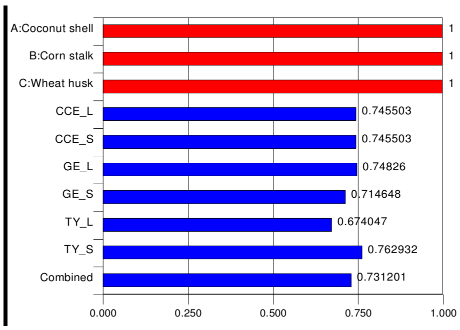

Fig. 5 Desirability for Optimal Solution

45.

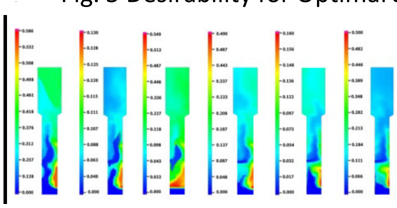

Fig. 6 Flow patterns transformation colored with particle volume fraction